Platinum Monolayer Electrocatalyst on Gold Nanostructures on Silicon for Photoelectrochemical Hydrogen Evolution

Joohong Kye,[†] Muncheol Shin,[†] Bora Lim,[†] Jae-Won Jang,[‡] Ilwhan Oh,[§] and Seongpil Hwang[†,*]

[†]Department of Chemistry, Myongji University, Yongin 449-728, Republic of Korea, [‡]Department of Physics, Pukyong National University, Busan 608-737, Republic of Korea, and [§]Department of Applied Chemistry, Kumoh National Institute of Technology, Gumi 730-701, Republic of Korea

ABSTRACT Pt monolayer decorated gold nanostructured film on planar p-type silicon is utilized for photoelectrochemical H_2 generation in this work. First, gold nanostructured film on silicon was spontaneously produced by galvanic displacement of the reduction of gold ion and the oxidation of silicon in the presence of fluoride anion. Second, underpotential deposition (UPD) of copper under illumination produced Cu monolayer on gold nanostructured film followed by galvanic exchange of less-noble Cu monolayer with more-noble $PtCl_6^{2-}$. Pt(shell)/Au(core) on p-type silicon showed the similar activity with platinum nanoparticle on silicon for photoelectrochemical hydrogen evolution reaction in spite of low platinum loading. From Tafel analysis, Pt(shell)/Au(core) electrocatalyst shows the higher area-specific activity than platinum nanoparticle on silicon demonstrating the significant role of underlying gold for charge transfer reaction from silicon to H^+ through platinum catalyst.

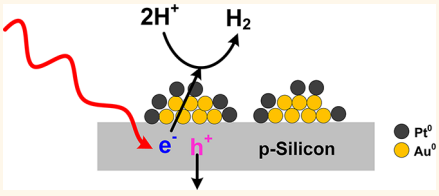

KEYWORDS: gold nanoparticles · silicon surfaces · galvanic displacement · galvanic exchange · underpotential deposition · photoelectrochemistry · solar fuel

Photoelectrochemical water splitting to produce hydrogen fuel from water and sunlight for emission-free and sustainable energy storage has drawn much interest because the rate of global energy use of fossil fuels has dramatically increased and the related environmental issues such as climate change demand more sustainable energy policy.[1−4] The electrodes for photoelectrochemical cell are composed of light-absorbing materials which have appropriate band-edge positions for the photoelectrochemical reduction of water. Among several semiconductors investigated as light-absorbing materials composing photoelectrochemical cells,[4] silicon (Si) is an earth-abundant, relatively low-cost material which is most widely used in current photovoltaics, with vast knowledge base and infrastructure. Although p-type silicon (p-Si) has suitable band gap for efficient sunlight collection and the conduction band edge position with respect to the electrochemical potential of water reduction, *i.e.*, hydrogen evolution reaction (HER), the sluggish kinetics of water electrolysis occurring at a silicon surface limit the efficiency of this reaction. A discontinuous layer of an electrocatalyst such as platinum is deposited to catalyze HER while maintaining photovoltages.[5] In addition, metallic nanoparticles with large surface area have been immobilized to enhance the kinetics of HER on planar silicon[6] and on silicon microwire.[7] The problem of high platinum content, however, has been one of obstacles for practical applications due to the high price and the limited world reserves of platinum. The main challenge is the development of cheap and stable electrocatalyst for photoelectrochemical hydrogen evolution. One approach in the development of HER catalyst is to enhance apparent kinetics of the low electrocatalytic activity of earth-abundant, nonprecious metal by increasing surface area.[8] Several groups reported attractive electrocatalysts for HER through this approach including bioinspired MoS_2[9] and Ni−Mo alloy,[10,11] with a nanostructured silicon pillar, and nanoporous NiMo alloy.[11]

Another approach in parallel with the nonprecious metal approach is advanced platinum-based electrocatalyst due to the higher activity for HER. Because of the high

* Address correspondence to shwang@mju.ac.kr.

Received for review April 8, 2013 and accepted June 10, 2013.

Published online June 10, 2013
10.1021/nn401720x

price and supply constraints, however, Pt-based catalysts must have high mass activities given by the higher fraction of exposed Pt atoms on the surface. In terms of the higher fraction of surface atoms, the Pt-monolayer approach is an attractive design of electrocatalysts having monolayer amount of Pt on a surface of non-Pt based metal core. In this approach, all Pt atoms exist on the surface of the nanoparticle achieving high mass activities. It has been one of the successful methods in developing electrocatalyst for oxygen reduction reaction (ORR) in fuel cell. Briefly, a monolayer of non-noble metal such as copper (Cu) is deposited at underpotential region followed by galvanic exchange of a monolayer of non-noble metal by more noble metal such as Pt under open-circuit condition.[12] Adzic *et al.* demonstrated the advantages of the monolayer approach in ORR including high utilization of Pt, enhanced activity, and long-term stability.[13−15] In addition to ORR, this monolayer approach has been applied to other reactions including oxidation of formic acid,[16] H_2 storage,[17] and HER.[18−20] The findings are interesting and may pave a new way to prepare electrocatalyst for HER in solar water splitting. Platinum nanoparticles on silicon consisting of various sizes and densities have been developed for photoelectrochemical HER.[20] To the best of our knowledge, however, the Pt-monolayer approach has not yet been reported for photoelectrochemical HER though Pt-monolayer may provide the same catalytic activity as Pt with very low contents.

Galvanic displacement is a spontaneous electrochemical reaction which is an efficient and attractive approach for the synthesis of metallic nanostructures on semiconductors.[21] In galvanic displacement, metal ions with a redox potential more positive than that of substrate are spontaneously reduced by the oxidation of the substrate itself upon immersion in the plating solution, without external power source or reducing agent. Because galvanic displacement is carried out with simple apparatus, this method provides an attractive alternative to commonly used sputtering or metal evaporation. For silicon, galvanic displacement of gold ions is typically carried out in fluoride containing plating solution where the oxidized substrate (SiO_2) is dissolved to keep supplying electrons by exposing unreacted silicon atoms to the solution.[21] Various gold structures including nanoparticles, nanostructure and film have been fabricated on semiconductor by galvanic displacement.[22,23] Recently, studies using fluoride-free plating solution were also reported to form ultrasmooth film, so-called self-limiting galvanic displacement.[24,25]

Herein we report the Pt monolayer decorated gold nanostructured film on planar p-Si (Pt/AuNF/Si) and their enhanced photoelectrochemical H_2 generation. Gold nanostructured film on silicon was spontaneously produced by galvanic displacement of the reduction of gold ion and the oxidation of silicon in the presence of fluoride anion. Then, copper monolayer on AuNF on Si was

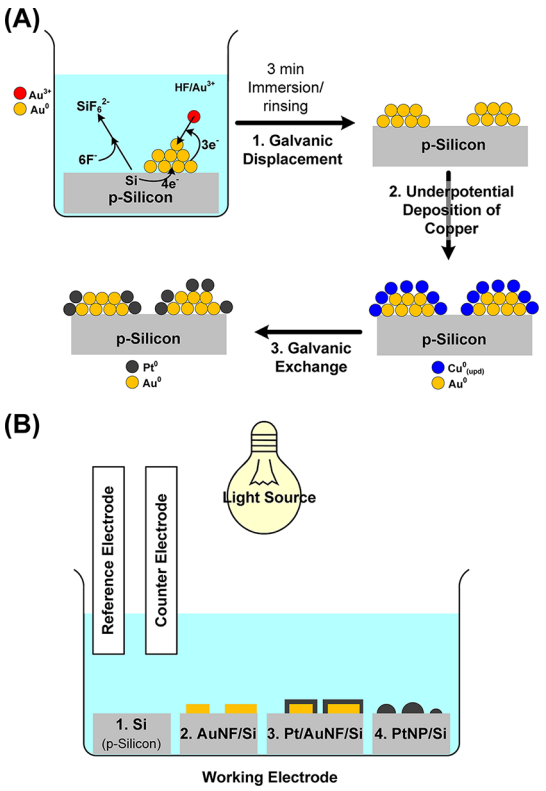

Scheme 1. (A) Schematic diagram of the fabrication of Pt monolayer decorated Au nanofilm on p-silicon. First, galvanic displacement occurs by immersion of a silicon substrate into a mixture of metal salt and HF. Metal salt, such as gold or platinum, are reduced concomitant with the oxidation of silicon. Second, monolayer thickness of copper is deposited underpotentially on Au nanofilm under illumination. Finally, Pt monolayer is galvanically deposited with labile copper monolayer by galvanic exchange. (B) Schematic diagram of measurement for photoelectrochemical H_2 generation on p-Si with various catalysts.

produced by underpotential deposition (upd) of copper under illumination by controlling external potential in the plating solution. The platinum submonolayer on AuNF was achieved by galvanic exchange of less-noble Cu monolayer with more-noble $PtCl_6^{2-}$ under open-circuit condition. Photoelectrochemistry of Pt(shell)/AuNF(core)/Si was investigated to measure the activity of platinum shell on silicon for photoelectrochemical hydrogen evolution reaction. The electrochemical active surface area (ESA) of deposited platinum was determined by hydrogen upd to confirm the relation between photoelectrochemical performance and surface area of Pt. From Tafel analysis, the area-specific activity of Pt(shell)/Au(core) electrocatalyst for HER was measured to demonstrate the role of underlying gold interface for charge transfer reaction from silicon to H^+ through platinum catalyst.

RESULTS AND DISCUSSION

Formation of Gold Nanostructured Film (AuNF) on Silicon by Galvanic Displacement and Deposition of Platinum Monolayer on AuNF by Galvanic Exchange. Scheme 1A outlines the procedure for the synthesis of Pt/AuNF/Si photocathode,

which begins with the synthesis of AuNF by electroless galvanic displacement with $AuCl_4^-$ and silicon in the presence of F^- ions. Cu monolayer is formed on AuNF by upd under external voltage under illumination of light. Then, Pt monolayer was formed by galvanic exchange of Cu UPD with $PtCl_6^{2-}$ under open circuit condition to produce Pt/AuNF/Si.

First, gold nanofilm was spontaneously deposited by galvanic displacement which occurs in 2 mM $HAuCl_4$ in the presence of HF for 3 min on p-type silicon. The spontaneous deposition can be described by the following two-half-cell reactions.

$$\text{anodic}: Si + 6HF \rightarrow SiF_6^{2-} + 6H^+ + 4e^-$$

$$\text{cathodic}: AuCl_4^- + 3e^- \rightarrow Au^0(s) + 4Cl^-$$

Au deposition in conjunction with corrosion of Si formed AuNF. Figure 1 shows the formation of nanostructured Au films (AuNF) on p-Si(100). SEM image reveals thin, homogeneous and discontinuous gold film on Si substrate with ligaments and holes of the order of 30−50 nm in diameter which is in accordance with previously reported results for galvanic displacement.[22,23]

To decorate AuNF with a Pt monolayer, the fabricated AuNF/Si served as working electrode for Cu upd and subsequent galvanic exchange. In the absence of illumination, cathodic current for Cu upd was not observed due to the absence of electrons in p-type Si.[26] Inset to Figure 2 shows the cyclic voltammograms (CVs) of AuNF/Si with and without copper ion in the electrolyte under illumination. The cathodic peaks at 0.180 V and at 0.011 V corresponding to the deposition of Cu upd on AuNF were observed demonstrating that Cu upd occurred by photoexcited electron upon illumination. In the bulk deposition realm, the deposition of Cu begins at −0.050 V. In the absence of Cu^{2+}, there is no faradic current as shown by the solid line demonstrating the Cu upd on AuNF/Si. After a Cu monolayer was deposited underpotentially on AuNF by linear sweep voltammetry as shown in Figure 2, potential was held at −0.05 V to minimize bulk deposition of Cu. Then, the Cu upd layer was galvanically exchanged with Pt under open-circuit condition by immersion of Cu/AuNF/Si into the solution containing 10 mM K_2PtCl_6 and 0.1 M $HClO_4$ for 3 min in the argon filled glovebag. As a control experiment, platinum nanoparticles on Si (PtNP/Si), a typical photocathode, was produced by galvanic displacement.

The number of Au sites and Pt sites available for electrochemical reaction was measured using Cu upd and hydrogen upd, respectively. The charge to deposit Cu upd on AuNF provides electroactive surface area (ESA) of exposed Au on Si using following equation.

$$ESA_{Au} = Q_{Cu}/(0.46A_{geo}) \quad (1)$$

where Q_{Cu} is the measured charge for Cu upd on AuNF; the correlation constant of 0.46 (mC/cm^2) represents

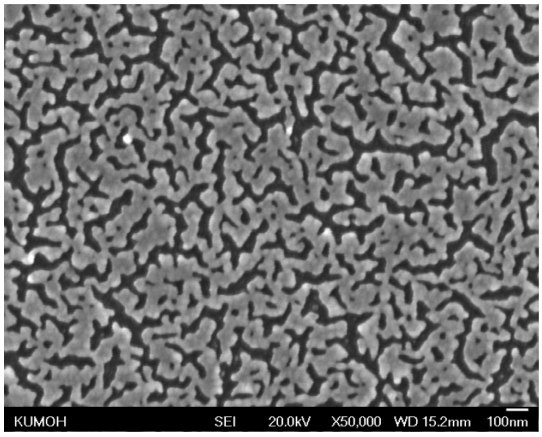

Figure 1. Nanostructured gold film (AuNF) on silicon by galvanic displacement imaged with scanning electron microscope.

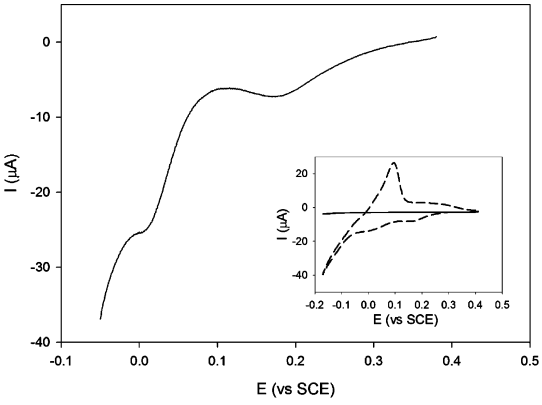

Figure 2. Linear sweep voltammogram for a AuNF/Si in an aqueous solution containing 5 mM $CuSO_4$ and 0.1 M H_2SO_4 under front side illumination. Inset shows CV for a AuNF/Si in 0.1 M H_2SO_4 with (dashed line) and without 5 mM $CuSO_4$ (solid line). Scan rate was 0.02 V/s.

the coulometric charge required to deposit Cu upd on Au(111).[27] A_{geo} represents the geometric area of electrode which is exposed to the solution. Cu upd both on AuNF/p-Si(100) shown in Figure 2 and on AuNF on highly doped n-type silicon (n^+-Si, ρ = 0.001−0.003 Ω·cm) shown in Supporting Information provides evidence that the values of ESA_{Au} were 0.83 cm^2 per 1 cm^2 Si (geometric area). The hydrogen adsorption/desorption is a powerful technique to determine the ESA of a Pt catalyst on Si.[27] Based on CVs on n^+-Si shown in Figure 3, ESA_{Pt} can be measured using the following equation

$$ESA_{Pt} = Q_H/(0.21A_{geo}) \quad (2)$$

where Q_H is the measured charge for H adsorption/desorption (H upd) upd on Pt; the correlation constant of 0.21 (mC/cm^2) represents the coulometric charge required to deposit H upd on Pt.[27] Because H upd was not observed even in the presence of illumination in the case of p-Si, highly doped n-type silicon was served as working electrode. It is worth mentioning that Pt^{2+} instead of Pt^{4+} might increase the coverage of exchanged

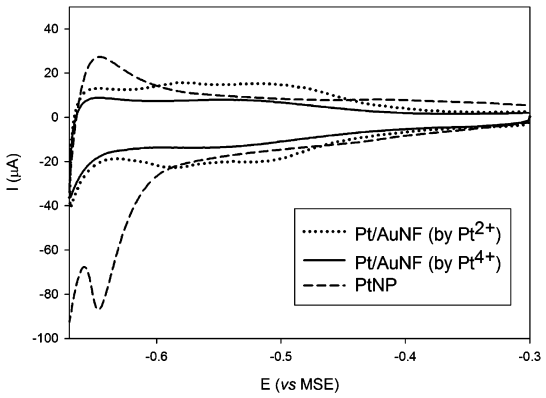

Figure 3. Cyclic voltammograms for H upd on a various Pt catalyst on n^+-Si in an aqueous solution containing 1 M H_2SO_4 without illumination. Scan rate = 0.05 V/s.

platinum by a factor of 2. H upd both on Pt(from Pt^{4+})-AuNF/n^+-Si(100), Pt(from Pt^{2+})AuNF/n^+-Si(100) and on PtNP/n^+-Si(100) shown in Figure 3 provides evidence that the values of ESA_{Pt} were 0.501, 0.820, and 1.78 cm^2 per 1 cm^2 Si (geometric area), respectively. Thus, coverages of Pt on AuNF from Pt^{4+} and Pt^{2+} ions were *ca.* 0.6 and 0.98 while ESA_{Pt} of PtNP is much larger owing to fine nanostructures. Surface areas of AuNF and Pt are summarized in Table 1. Interestingly, the high coverage Pt/AuNF/Si showed substantial dark current which is similar to the Pt electrode. The photovoltage, however, is decreased to just *ca.* 50 mV (see Figure S2 in Supporting Information). Because other conditions are exactly same in both cases, difference in photovoltage should originate from Pt coverage. At the current stage, the reason why the high-coverage Pt/Au/Si exhibits lower photovoltage is unclear. One explanation is that the adsorption of Pt on Au seems to shift Fermi level of Pt/Au by charge transfer that was reported experimentally by Plasmon shift of core−shell nanoparticles.[28] This can somehow affect the interface energetics and attenuate the pinch-off effect. Therefore, the interface between Pt/AuNF/Si and electrolyte may be considered as three inhomogeneous barrier heights of Electrolyte/Si, Au/Si (Pt unmodified AuNF/Si) and (Pt/Au)/Si (Pt modified AuNF/Si). As the number of (Pt/Au)/Si junction increases, the semiconductor/electrolyte interface no longer dominates the junction energetics but (Pt/Au)Si substantially contributes to the energetics. For this reason, galvanic exchange using Pt^{4+} will be discussed in the following section.

Photoelectrochemical Study of Pt/AuNF/Si Electrode for Hydrogen Evolution Reaction. Photoelectrochemical H_2 generation of various catalysts was measured under illumination as shown in Scheme 1B.[29,30] Figure 4 shows current density (J)-electrode potential (*E*) measurements for H_2 generation on p-Si with various metal films under illumination in a stirred aqueous solution containing H_2SO_4 and 0.5 M K_2SO_4 (pH 1). A calibrated halogen lamp illuminates the photocathode surface with 100 mW/cm^2 simulated solar radiance. Figure 4 shows that the bare planar Si (dash-dot line) exhibited a very small photocurrent for H_2 generation

TABLE 1. ESA Data (cm^2 per 1 cm^2 Si) of Gold and Platinum on the Different Electrodes

sample	ESA_{Au}	ESA_{Pt}
AuNF	0.83	
Pt(Pt^{4+})/AuNF		0.50
Pt(Pt^{2+})/AuNF		0.82
PtNP		1.78

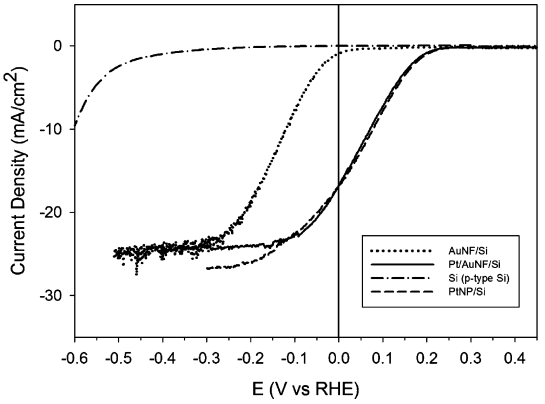

Figure 4. Photoelectrochemical H_2 generation on planar p-type Si electrodes with various catalyst under illumination in a stirred solution of H_2SO_4 + 0.5 M K_2SO_4 (pH 1). Scan rate was 0.02 V/s.

until *E* reached −0.5 V because without an electrocatalyst present on the Si surface, electron transfer from the Si surface to H^+ was very slow. In contrast, the AuNF/Si photocathode generated a much higher photocurrent (dotted line in Figure 4) at a lower overpotential. In the presence of Pt on AuNF/Si, photocathode demonstrates the enhanced photocurrent for H_2 generation due to the facile reduction of hydrogen as shown by the solid line in Figure 4. For example, to reach a current density of 10 mA/cm^2 corresponding to the hydrogen production rate of ∼0.05 μmol/s, the electrode potential is as positive as 0.071 V on Pt/AuNF/Si as compared with −0.120 V on AuNF/Si, demonstrating the improved catalysis with the cathodic shift of ∼0.191 V. For the same current density of 10 mA/cm^2, the potential on Pt nanoparticle modified p-Si (PtNP/Si) is a little positive, 0.078 V. The small overpotential for HER of Pt/AuNF/Si exhibits that catalytic effect of Au clusters on p-Si is enhanced by the adsorption of atomic layer of platinum by galvanic displacement similar to PtNP. It is also worth mentioning that saturation photocurrent of Pt/AuNF/Si is *ca.* 11% smaller than that of Si indicating that larger AuNF absorbed and/or reflected some of the incident light. Though previous works by other researchers showed that shadowing loss by the catalyst nanoparticles was negligible owing to small size of nanoparticles,[31] larger AuNF with higher coverage probably reduces the incident light power. The onset potential (E_{os}) and the light-limited photocurrent density (J_{Ph}) at the incident light intensity of 100 mW/cm^2 for the best electrodes with various catalysts

are listed in Table 2. Overall, the photoelectrochemical efficiency of Pt/AuNF/Si on HER is close to that of PtNP/Si and is in the order PtNP/Si ≈ Pt/Au/Si ≫ Au/Si ≫ Si.

The higher activity of Pt/AuNF/Si for HER may originate from either geometric effect (surface area of Pt) or electronic effect (the higher area-specific activity). A reduction in overpotential is achieved either by increasing the surface area of electrocatalyst (geometric effect) or by a modification of the nature of electrocatalyst (electronic effect). It is clear that the evaluation of catalysts by simple comparison of overpotentials is not adequate because exposed surface areas of PtNP, where rough hemispheres were observed (Figure S3), differ from that of Pt/AuNF (Figure 1). Therefore, the geometric factor and the electronic factor must be considered separately in evaluating electrocatalyst. First, The ESA_{Pt} values per 1 cm^2 Si of PtNP and Pt/AuNF were 1.78 and 0.501 cm^2 as listed in Table 1, respectively. The ESA_{Pt} value of PtNP is *ca.* 3.5 times larger than that of Pt/AuNF which might be attributed to three-dimensional fine structures of PtNP. AFM images also confirmed the larger surface area of PtNP compared with Pt/AuNF (figure not shown). Therefore, the surface area of Pt catalyst is not the origin of the higher activity of Pt/AuNF/Si due to the smaller ESA of Pt. It is worth mentioning that Pt by galvanic exchange covers only *ca.* half of AuNF surface area because the surface area of AuNF per 1 cm^2 Si calculated by the charge of Cu UPD was 0.83 cm^2. Although using Pt^{2+} instead of Pt^{4+} increased the Pt coverage close to full coverage, the photoelectrochemistry of such high-coverage Pt electrodes was deteriorated. Second, a Tafel analysis, the plot of η *vs* log i, was applied to voltammogram of each sample on n^+-Si to evaluate the electrocatalytic activity of Pt in the absence of light irradiation where the light process can be eliminated.[4] The overpotential (η) is related to the reaction rate by Tafel equation,

$$\eta = b \ln \frac{I}{I_0} \quad (3)$$

where b is Tafel slope and I_0 is the exchange current. I_0 or the normalized exchange current density (J_0) is used to compare the activity of electrodes because the exchange current density is the rate of reaction at equilibrium or at the reversible potential (the overpotential is zero). J_0, however, is an extensive quantity, which depends on the extension of the true surface area. On the other hand, the Tafel slope b is an intensive quantity, which does not depend on the surface area and accounts for electronic factors or reaction mechanism of catalyst. Comparison of Tafel plots in the absence of irradiation as shown in Figure 5 provides insight into the origin of different HER activities on various surfaces. From a simple Tafel analysis on the rising portion of the CVs, Tafel slopes were −56 mV/dec and −67 mV/dec for Pt/AuNF/Si and PtNP/Si, respectively. Concomitantly, the J_0 values for Pt/AuNF/Si and PtNP/Si were −3.78 and −3.18. Because J_0 is expressed in terms of geometric area, the higher J_0 value on PtNP/Si compared to that on Pt/AuNF/Si might be a result of larger surface area of PtNP as observed in ESA_{Pt} comparison. Tafel slope of Pt/AuNF/Si increased compared with PtNP/Si indicating the enhancement by the electronic effect of Pt submonolayer on AuNF. There are two possible reasons for this enhancement. One is a strain effect on the Pt overlayer on AuNF[32] which could shift the Pt d-band center. The other is the interfacial barrier layer such as silicon oxide between Si surface and PtNP which suppresses charge transport and decreases the Tafel slope of PtNP/Si.[10] Because such barrier layer does not exist at the interface between AuNF and Si surface,[23] the charge transport through Pt/AuNF/Si is faster than PtNP/SiO_2/Si, increasing the Tafel slope. Further investigation of Pt/AuNF/Si for the best trade-off between high catalytic activity and photovoltage is beyond the scope of the present paper but would be useful for the understanding and development of HER catalyst. In contrast, a Tafel slope of −110 mV/dec similar to reported value of −120 mV/dec[33] was obtained for AuNF/Si demonstrating that HER occurs on AuNF through different reaction mechanism or different electronic activity compared to both Pt/AuNF/Si and PtNP/Si. Overall, Pt monolayer on AuNF enhances the catalytic activity similar to PtNP because underlying gold influences the kinectics of monatomic Pt layer for HER by

TABLE 2. Comparison of electrode parameters for photoelectrochemical H_2 evolving photocathodes with various catalysts

sample	AuNF	Pt/AuNF	PtNP
E_{os} (mV)	137	249	252
J_{Ph} (mA/cm^2)	24.5	24.4	26.6

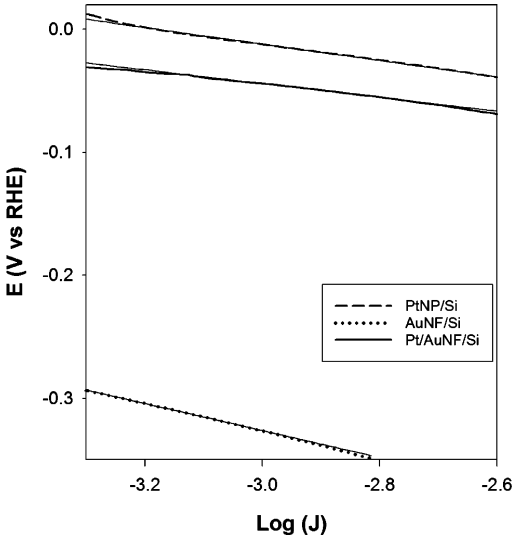

Figure 5. Tafel plots of the HER activities on planar n^+-Si electrodes with various catalyst in the absence of illumination in a solution of H_2SO_4 + 0.5 M K_2SO_4 (pH 1).

the strain effect or the fast charge transfer due to the absence of the interfacial oxide layer in the dark.

CONCLUSIONS

Monoatomic platinum overlayer on nanostructured gold film on p-silicon has been successfully deposited by galvanic exchange. First, nanostructure gold film was spontaneously produced by galvanic displacement of the reduction of gold ion and the oxidation of silicon in the presence of fluoride ions. Second, underpotential deposition of less-noble copper on AuNF under illumination forms the monatomic copper layer on AuNF. Spontaneous exchange of monatomic copper layer with platinum ions produced Pt/AuNF/Si for HER. Pt/AuNF/Si showed the similar activity with PtNP/Si. From Tafel analysis and analysis of surface area, the area-specific activity of Pt/AuNF/Si is higher than PtNP/Si while surface area of Pt on Pt/AuNF is smaller than that of PtNP/Si. Therefore, it is reasonable to suggest that modification of metal supporter with monatomic platinum could be potentially good replacement for pure platinum nanoparticles.

EXPERIMENTAL METHODS

Chemicals and Reagents. All chemicals were purchased from Sigma-Aldrich and used as received. Ultrapure water (>18 MΩ) from a Millipore Milli-Q purification system was used throughout this work. All glassware and electrochemical cells were cleaned with Nochromix (Godax Lab., Inc.) cleaning solution and rinsed with ultrapure water.

Fabrication of AuNF/Si and PtNP/Si Photocathode. Metal nanoparticles are produced by galvanic displacement in HF-based solution containing metal salt. A p-type Si (100) wafer (Wafer World, Inc.; ~10 Ω·cm; B-doped) or highly doped n-type Si (100) (n^+-Si, ρ = 0.001−0.003 Ω·cm) is degreased by rinsing with acetone, isopropyl alcohol, and ultrapure deionized water (DIW) in sequence. Backside ohmic contact is formed by depositing annealed Al ohmic layer onto the HF-treated Si wafer. For measurements in stirred solutions, the backside Al ohmic metal is first electrically connected to a Cu wire using Ag conductive adhesive. The Cu wire is threaded into a glass tube (6 mm o.d.). Backside contact area is electrically sealed using an epoxy resin (Hysol 1C). The front side of the Si sample is painted with another type of epoxy resin (Hysol 9460) except the very area (0.05−0.20 cm^2) that is defined as projected area of photocathode. The assembly is cured at room temperature overnight before use. An optical image of each sample was taken with a scanner (HP Scanjet G2410) and analyzed with Image J software to determine the active electrode surface area.

To synthesize metal nanoparticles on silicon, planar Si sample is first immersed in 0.4 M HF for 3 min to remove surface oxide. Gold nanoparticle (AuNF) and Pt NP are deposited by immersion of planar Si into a solution of 0.5 M HF for 3 min with 2 mM $HAuCl_4$ and 1 mM K_2PtCl_6, respectively. Then, Si substrate is rinsed with DIW, and dried with N_2. To deposit Pt shell, a Cu monolayer is deposited underpotentially on AuNF by linear sweep voltammetry holding the potential at −0.05 V under illumination. Then, the Cu upd layer is galvanically exchanged with Pt under open-circuit condition by immersion of Cu/AuNF/Si into the solution containing 10 mM K_2PtCl_6 (or K_2PtCl_4) and 0.1 M $HClO_4$ for 3 min in the argon filled glovebag.

Photoelectrochemical Measurements. For measurements in stirred solutions, a 100-mL round-bottomed flask (RBF) is used, where a stir bar is rotated at 500−1000 rpm by a magnetic stirrer as described elsewhere.[15,16] The sealed Si photocathode is placed at the center of the RBF, along with a photodiode, a Pt counter electrode, and a standard calomel reference electrode (SCE). The entire cell is immersed into a transparent water bath, which minimizes the focusing of illuminating light by the RBF and keeps the solution temperature constant. For illumination source, a halogen lamp is used, the intensity of which is calibrated to 100 mW/cm^2 by a Si photodiode (Hamamatus; model S2386-18K). Electrolyte solution is prepared by adding concentrated H_2SO_4 into 0.5 M K_2SO_4 along with pH measurement. All measurements are conducted in three-electrode configuration using a CHI 660D potentiostat. No other corrections for the polarization curves were performed (*i.e.*, the data were not corrected for IR drop or mass-transport).

Conflict of Interest: The authors declare no competing financial interest.

Acknowledgment. S. Hwang acknowledges the support from Basic Science Research Program through the National Research Foundation of Korea (NRF) funded by the Ministry of Education, Science and Technology (2012R1A1A2006038). S. Hwang thanks Dr. Jong-Seong Bae in Korea Basic Science Institute (KBSI Busan) for the XPS analysis.

Supporting Information Available: CV of Cu upd on AuNF/n^+-Si, photoelectrochemistry of Pt(by Pt^{2+})/AuNF/Si, SEM image of PtNP/Si, X-ray photoelectron spectra of substrates are reported. This material is available free of charge *via* the Internet at http://pubs.acs.org.

REFERENCES AND NOTES

1. Turner, J. A. Sustainable Hydrogen Production. *Science* **2004**, *305*, 972–974.
2. Bard, A. J.; Fox, M. A. Artificial Photosynthesis: Solar Splitting of Water to Hydrogen and Oxygen. *Acc. Chem. Res.* **1995**, *28*, 141–145.
3. Heller, A. Conversion of Sunlight into Electrical Power and Photoassisted Electrolysis of Water in Photoelectrochemical Cells. *Acc. Chem. Res.* **1981**, *14*, 154–162.
4. Walter, M. G.; Warren, E. L.; McKone, J. R.; Boettcher, S. W.; Mi, Q.; Santori, E. A.; Lewis, N. S. Solar Water Splitting Cells. *Chem. Rev.* **2010**, *110*, 6446–6473.
5. Nakato, Y.; Yano, H.; Nishiura, S.; Ueda, T.; Tsubomura, H. Hydrogen Photoevolution at p-Type Silicon Electrodes Coated with Discontinuous Metal Layers. *J. Electroanal. Chem.* **1987**, *228*, 97–108.
6. Dominey, R. N.; Lewis, N. S.; Bruce, J. A.; Bookbinder, D. C.; Wrighton, M. S. Improvement of Photoelectrochemical Hydrogen Generation by Surface Modification of p-Type Silicon Semiconductor Photocathodes. *J. Am. Chem. Soc.* **1982**, *104*, 467–482.
7. Boettcher, S. W.; Warren, E. L.; Putnam, M. C.; Santori, E. A.; Turner-Evans, D.; Kelzenberg, M. D.; Walter, M. G.; McKone, J. R.; Brunschwig, B. S.; Atwater, H. A.; *et al.* Photoelectrochemical Hydrogen Evolution Using Si Microwire Arrays. *J. Am. Chem. Soc.* **2011**, *133*, 1216–1219.
8. Tran, P. D.; Wong, L. H.; Barber, J.; Loo, J. S. C. Recent Advances in Hybrid Photocatalysts for Solar Fuel Production. *Energy Environ. Sci.* **2012**, *5*, 5902–5918.
9. Hou, Y.; Abrams, B. L.; Vesborg, P. C. K.; Björketun, M. E.; Herbst, K.; Bech, L.; Setti, A. M.; Damsgaard, C. D.; Pedersen, T.; Hansen, O.; *et al.* Bioinspired Molecular Co-catalysts Bonded to a Silicon Photocathode for Solar Hydrogen Evolution. *Nat. Mater.* **2011**, *10*, 434–438.
10. McKone, J. R.; Warren, E. L.; Bierman, M. J.; Boettcher, S. W.; Brunschwig, B. S.; Lewis, N. S.; Gray, H. B. Evaluation of Pt, Ni, and Ni−Mo Electrocatalysts for Hydrogen Evolution on Crystalline Si Electrodes. *Energy Environ. Sci.* **2011**, *4*, 3573–3583.
11. Reece, S. Y.; Hamel, J. A.; Sung, K.; Jarvi, T. D.; Esswein, A.; Pijpers, J. J. H.; Nocera, D. G. Wireless Solar Water Splitting Using Silicon-Based Semiconductors and Earth-Abundant Catalysts. *Science* **2011**, *334*, 645–648.

12. Brankovic, S. R.; Wang, J. X.; Adzic, R. R. Metal Monolayer Deposition by Replacement of Metal Adlayers on Electrode Surface. *Surf. Sci.* **2001**, *474*, L173–L179.
13. Zhang, J.; Lima, F. H. B.; Shao, M. H.; Sasaki, K.; Wang, J. X.; Hanson, J.; Adzic, R. R. Platinum Monolayer on Nonnoble Metal-Noble Metal Core-Shell Nanoparticle Electrocatalysts for O_2 Reduction. *J. Phys. Chem. B* **2005**, *109*, 22701–22704.
14. Zhang, J.; Sasaki, K.; Sutter, E.; Adzic, R. R. Stabilization of Platinum Oxygen-Reduction Electrocatalysts Using Gold Clusters. *Science* **2007**, *315*, 220–222.
15. Adzic, R. R.; Zhang, J.; Sasaki, K.; Vukmirovic, M. B.; Shao, M.; Wang, J. X.; Nilekar, A. U.; Mavrikakis, M.; Valerio, J. A.; Uribe, F. Platinum Monolayer Fuel Cell Electrocatalysts. *Top. Catal.* **2007**, *46*, 249–262.
16. Wang, S.-H.; Zhang, H. -X.; Cai, W.-B. Mimetic Underpotential Deposition Technique Extended for Surface Nanoengineering of Electrocatalysts. *J. Power Sources* **2012**, *212*, 100–104.
17. Sheridan, L. B.; Czerwiniski, J.; Jayaraju, N.; Gebregziabiher, D. K.; Stickney, J. L.; Robinson, D. B.; Soriaga, M. P. Electrochemical Atomic Layer Deposition (E-ALD) of Palladium Nanofilms by Surface Limited Redox Replacement (SLRR), with EDTA Complexation. *Electrocatalysis* **2012**, *3*, 96–107.
18. Liu, Y.; Mustain, W. E. Evaluation of Tungsten Carbide as the Electrocatalyst Support for Platinum Hydrogen Evolution/oxidation Catalysts. *Int. J. Hydrogen Energy* **2012**, *37*, 8929–8938.
19. Hsu, I. J.; Kimmel, Y. C.; Jiang, X.; Willis, B. G.; Chen, J. G. Atomic Layer Deposition Synthesis of Platinum−tungsten Carbide Core−shell Catalysts for the Hydrogen Evolution Reaction. *Chem. Commun.* **2012**, *48*, 1063–1065.
20. Lombardi, I.; Marchionna, S.; Zangari, G.; Pizzini, S. Effect of Pt Particle Size and Distribution on Photoelectrochemical Hydrogen Evolution by p-Si Photocathodes. *Langmuir* **2007**, *23*, 12413–12420.
21. Carraro, C.; Maboudian, R.; Magagnin, L. Metallization and Nanostructuring of Semiconductor Sufaces by Galvanic Displacement Processes. *Surf. Sci. Rep.* **2007**, *62*, 499–525.
22. Magagnin, L.; Maboudian, R.; Carraro, C. Gold Deposition by Galvanic Displacement on Semiconductor Surfaces: Effect of Substrate on Adhesion. *J. Phys. Chem. B* **2002**, *106*, 401–407.
23. Sayed, S. Y.; Wang, F.; Malac, M.; Meldrum, A.; Egerton, R. F.; Buriak, J. M. Heteroepitaxial Growth of Gold Nanostructures on Silicon by Galvanic Displacement. *ACS Nano* **2009**, *3*, 2809–2817.
24. Gutés, A.; Carraro, C.; Maboudian, R. Ultrasmooth Gold Thin Films by Self-Limiting Galvanic Displacement on Silicon. *ACS Appl. Mater. Interfaces* **2011**, *3*, 1581–1584.
25. Fabre, B.; Hennous, L.; Ababou-Girard, S.; Meriadec, C. Electroless Patterned Assembly of Metal Nanoparticles on Hydrogen-Terminated Silicon Surfaces for Applications in Photoelectrocatalysis. *ACS Appl. Mater. Interfaces* **2013**, *5*, 338–343.
26. Kobayashi, K.; Harraz, F. A.; Izuo, S.; Sakka, T.; Ogata, Y. H. Microrod and Microtube Formation by Electrodeposition of Metal into Ordered Macropores Prepared in p-Type Silicon. *J. Electrochem. Soc.* **2006**, *153*, C218–C222.
27. Herrero, E.; Buller, L. J.; Abruna, H. D. Underpotential Deposition at Single Crystal Surfaces of Au, Pt, Ag and Other Materials. *Chem. Rev.* **2001**, *101*, 1897–1930.
28. Pande, S.; Ghosh, S. K.; Praharaj, S.; Panigrahi, S.; Basu, S.; Jana, S.; Pal, A.; Tsukuda, T.; Pal, T. Synthesis of Normal and Inverted Gold-Silver Core-Shell Architectures in α-Cyclodextrin and Their Applications in SERS. *J. Phys. Chem. C* **2007**, *111*, 10806–10813.
29. Oh, I.; Kye, J.; Hwang, S. Fabrication of Metal-Semiconductor Interface in Porous Silicon and Its Photoelectrochemical Hydrogen Production. *Bull. Korean Chem. Soc.* **2011**, *32*, 4392–4396.
30. Oh, I.; Kye, J.; Hwang, S. Enhanced Photoelectrochemical Hydrogen Production from Silicon Nanowire Array Photocathode. *Nano Lett.* **2012**, *12*, 298–302.
31. Heller, A. Hydrogen-Evolving Solar Cells. *Science* **1984**, *223*, 1141.
32. Wolfschmidt, H.; Bussar, R.; Stimming, U. Charge Transfer Reactions at Nanostructured Au(111) Surfaces: Influence of the Substrate Material on Electrocatalytic Activity. *J. Phys.: Condens. Matter* **2008**, *20*, 374127.
33. Perez, J.; Gonzalez, E. R.; Villullas, H. M. Hydrogen Evolution Reaction on Gold Single-Crystal Electrodes in Acid Solutions. *J. Phys. Chem. B* **1998**, *102*, 10931–10935.